


NGU Report 2014.049
Mapping of fracture zones using resistivity
method between islands at Arsvågen, Bokn
municipality, Rogaland - ROGFAST project

Report no.: 2014.049		ISSN 0800-3416	Grading: Open
Title: Mapping of fracture zones using resistivity method between islands at Arsvågen, Bokn municipality, Rogaland - ROGFAST project			
Authors: Georgios Tassis, Einar Dalsegg, Bjørn Eskil Larsen & Jan Steinar Rønning		Client: Statens Vegvesen ROGFAST project, Statens vegvesen Vegdirektoratet and NGU	
County: Rogaland		Commune: Bokn	
Map-sheet name (M=1:250.000) Haugesund		Map-sheet no. and -name (M=1:50.000) 1113-II Skudeneshavn	
Deposit name and grid-reference: Arsvågen		Number of pages: 23	Price (NOK): 150,-
Fieldwork carried out: October 2014		Date of report: 31.11.2014	Project no.: 329500 / 341500
			Person responsible: 
<p>Summary:</p> <p>This survey was carried out in cooperation with the Norwegian Public Roads Administration (Statens Vegvesen) to aid and supplement the construction of a major tunnel in Arsvågen, Rogaland. Essentially, this work follows up ROGFAST project which also included resistivity measurements at the island of Kvitsøy just south of the new survey area. It is also in close connection to another NGU project which tested the efficiency of 2D resistivity method in marine environments. Our aim is to utilize the results of the aforementioned report in order to be able to discard the sea water effect and thereafter detect and characterize possible fracture zones which may affect the stability of the tunnel construction at hand.</p> <p>We have conducted resistivity measurements along a 1600 meter long profile using multiple gradient array with 5 meter electrode spacing and sea-bottom electrode configuration. In addition, the first half of the profile (800 m) has also been measured with two additional arrays (pole-dipole and dipole-dipole) as well as with both floating and sea-bottom electrode mode for all arrays. In marine environments, the presence of very conductive seawater introduces the problem of current loss since electricity prefers to travel through saline water instead of the highly resistive bedrock. Prior modeling has shown that 2D resistivity measurements can work successfully under strict prerequisites which include detailed knowledge of the resistivity properties and geometry of the sea water areas themselves.</p> <p>In this study we have conducted all measurements according to these conditions since our profile crosses 5 marine straits. Detailed sea water resistivity and depth measurements have been conducted and subsequently utilized in data processing. However, the highly conductive sea water (resistivity 0.20 Ohm·m) and strongly resistive bedrock (5000 Ohm·m and more) have rendered our measurements extremely noisy and hard to process.</p> <p>Unfortunately the inherent restrictions of marine ERT combined with the extreme difference in resistivity between bedrock and seawater in the area makes it near impossible to extract any solid conclusions about possible fracture zones wherever seawater is present and/or in the near vicinity. Such areas are dominated by artificial effects i.e. false anomalies which mask the underground resistivity setting and prohibiting us from reaching any conclusion. On the other hand, the parts of the profile where electrodes are positioned in dry land are more reliable and we can safely suggest that they don't reveal any major fracture zones.</p> <p>To sort out whether there are fracture zones in bedrock under the investigated straits at Årvågen or not, the NGU recommends to perform refraction seismic measurements. To overcome 3D effects on the resistivity data, NGU will perform new modeling and inversion when appropriate software is available.</p>			
Keywords: Geophysics	2D Resistivity		Marine
Fracture zones	Tunnel		
			Scientific report

CONTENTS

1. INTRODUCTION	4
2. CHALLENGES AT THE SURVEY AREA.	5
2.1 Area description.....	5
2.2 Challenges	6
3. METHOD DESCRIPTION	7
3.1 Method outline.....	7
3.2 Resistivity data acquisition.....	9
3.3 Measurement parameters.....	11
3.4 Seawater conductivity and depth measurements.....	11
3.5 Inversion	13
4. RESULTS AND DISCUSSION	13
5. CONCLUSIONS.....	17
6. REFERENCES	18
7. APPENDIX 1, Station coordinates	23

FIGURES

Figure 1: Geological setting of the study area at Arsvågen - 1:250.000 NGU Haugesund Bedrock Map (Ragnhildstveit et al. 1998).	5
Figure 2: Geographical positioning of the profile with respect to the scheduled tunnel route. .	6
Figure 3: Electrode array for measuring the ground resistivity (modified by Todd 1959).	8
Figure 4: Sequence of measurements and structuring of a pseudosection (Dahlin 1993).	8
Figure 5: Diagram of measuring procedure. When measurements with four cables are terminated the first cable is moved at the end of the outlay to continue measurements as far as it is required (From Dahlin 1993).	9
Figure 6: Floating electrode mode with the use of empty canisters along a strait in Arsvågen.	10
Figure 7: Sea-bottom electrode mode with the cable sinking to the sea bottom on its own weight.	10
Figure 8: Field measurements of sea water depth and conductivity/resistivity.	12
Figure 9: Modeled resistivity with topography for multiple gradient array on sea-bottom electrode mode (top side) and floating electrode mode (bottom side). Inversion parameters: Robust data inversion/Fast module, V/H filter = 1.5.	19
Figure 10: Modeled resistivity with topography for dipole-dipole array on sea-bottom electrode mode (top side) and floating electrode mode (bottom side). Inversion parameters: Robust data inversion/Fast module, V/H filter = 1.5.	20
Figure 11: Modeled resistivity with topography for pole-dipole array on sea-bottom electrode mode (top side) and floating electrode mode (bottom side). Inversion parameters: Robust data inversion/Fast module, V/H filter = 1.5.	21
Figure 12: Modeled resistivity with topography for multiple gradient array on sea-bottom electrode mode with V/H filter equal to 1.0 (top side) and with V/H filter equal to 1.5 (bottom side). Inversion parameters: Robust data inversion/Fast module.....	22

1. INTRODUCTION

This survey was carried out in cooperation with the Norwegian Public Roads Administration (Statens Vegvesen) to aid and supplement the construction of a major tunnel in Arsvågen, Rogaland. Essentially, this work follows up ROGFAST project which also included resistivity measurements at the island of Kvitsøy just south of the new survey area (Dalsegg 2012). It is also in close connection to another NGU report which tested the efficiency of 2D resistivity method in marine environments (Tassis et al. 2013). Our aim is to utilize the results of the aforementioned report in order to be able to discard the sea water effect and thereafter detect and characterize possible fracture zones which may affect the stability of the tunnel construction at hand. This research project is financed by Statens vegvesen ROGFAST project, Statens Vegvesen/Road directorate and the Geological survey of Norway.

The NGU has applied the 2D Resistivity method in the detection of fracture zones in bedrock which might be a challenge for technical structures for more than 10 years (Rønning, 2003; Dalsegg, 2012, Rønning et al. 2014). Lately, the demand for testing the efficiency of 2D Resistivity in marine environments has increased, in relation to the construction of underwater tunnels in western Norway and the need to detect any weak zones present that engineers ought to know about beforehand. Therefore modeling had to be expanded from dry land conditions (Reiser et al., 2009; Rønning et al., 2009) to marine environments (Tassis et al., 2013). The latter has unveiled that marine 2D Resistivity measurements are possible under several strict rules. More specifically, modeling has shown that multiple gradient and dipole-dipole should be preferred over other arrays and that sea bottom electrode mode i.e. a survey where electrodes are attached to the sea bottom instead of floating, gives far better results. Furthermore, when using sea bottom electrode mode to conduct resistivity measurements, the maximum sea water depth should be less than 10 meters deep. In our case, we have focused on the multiple gradient array since dipole-dipole has a low signal to noise ratio with electrodes attached to the sea bottom due to the fact that the maximum depth in the region is no more than 5 meters (~4,6 meters). This fact certifies that 2D resistivity method is applicable in Arsvågen. To test the performance of other configurations, parts of the profile were measured using pole-dipole and dipole-dipole configurations with floating and seabottom electrodes.

After certifying the theoretical feasibility of the study in marine areas, we have conducted resistivity measurements along a 1600 meter long profile by inserting electrical current into the ground and subsequently measuring the resulting potential difference with the use of electrodes. By changing the distance and positioning of both the current and potential electrodes we were able to map the electrical properties of the underground and compile vertical tomographies. By tomographies we refer to 2 dimensional distribution of resistivity of the underground after proper processing. Assigning the resulting resistivities to known geological formations we were able to create a model of the underground geology for our study area which is both qualitative and quantitative. This enables us to predict and outline features such as fracture zones. However, the presence of very conductive seawater introduces the problem of current loss since electricity prefers to travel through it instead of the more resistive bedrock. Modeling has also shown that 2D resistivity measurements can be interpreted successfully only with detailed knowledge of the resistivity properties and geometry of the sea water areas themselves.

The full profile has been measured with the Lund setting (Dahlin 1993) with multiple gradient array and by using sea-bottom electrodes wherever seawater was present. This particular

setting has been proven to give the best results in marine ERT prospecting. However, other arrays such as dipole-dipole could also prove helpful when certain conditions are met. The northern half of the profile (800 meters) crosses three seawater straits and we found this environment to be very suitable for testing the knowledge that we have already acquired through marine ERT modeling. In this sense, pole-dipole and dipole-dipole arrays have been utilized additionally to multiple gradient while sea-bottom and floating electrode mode has been employed to all arrays. This way we have produced six additional testing data sets which will be presented in this report.

2. CHALLENGES AT THE SURVEY AREA.

2.1 Area description

No geological mapping was done during this project. Instead large scale geological investigations for the entire ROGFAST project were done by Solli (2014). According to the aforementioned NGU report and the N250 bedrock maps the Bokn area consists of dioritic gneiss, which is a part of the proterozoic western gneiss region. The expected resistivity for massive diorites in Norway according to measurements performed by Elvebakk (2011) is around 5000 Ωm. Less massive and fractured rocks will subsequently have lower resistivities.

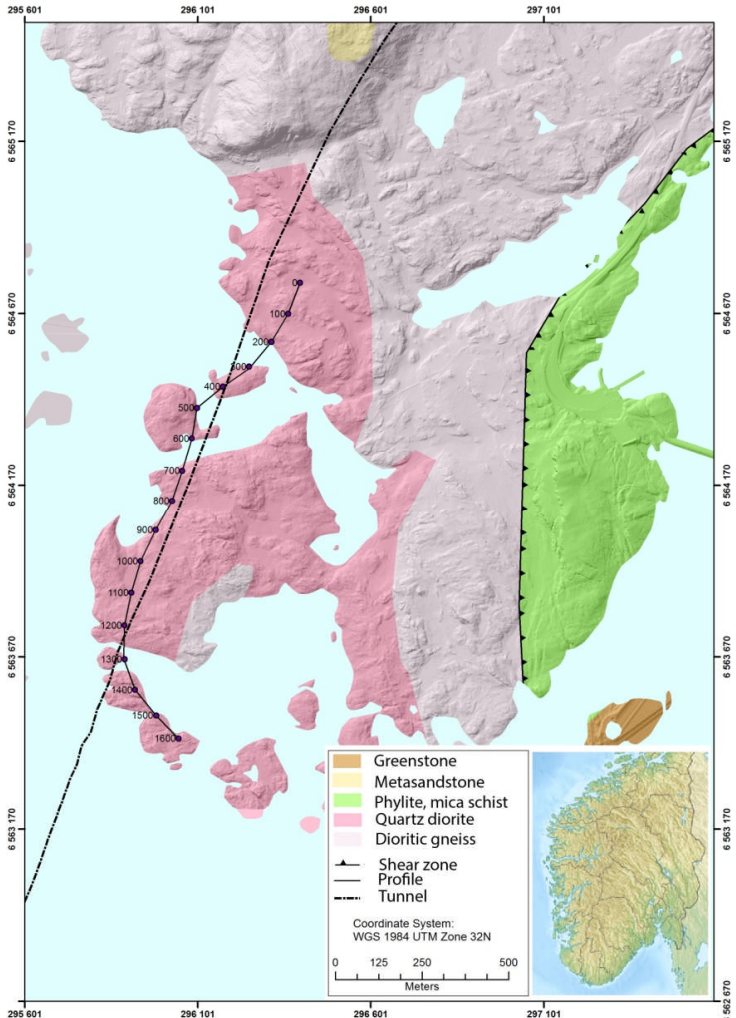


Figure 1: Geological setting of the study area at Arsvågen - 1:250.000 NGU Haugesund Bedrock Map (Ragnhildstveit et al. 1998).

The Bokn area is sandwiched between the Karmøy ophiolite in the west and the Viste nappe, which is a part of the lower allochthon of the Caledonian orogeny (**figure 1**). The thrust-zone separating the Viste nappe and the proterozoic bedrock is around 1 km east of the investigated area. On the other hand, the contact to the Karmøy ophiolite to the west is interpreted to be a west dipping subvertical normal fault with N-S striking. The contact is not exposed on land but runs along the strait separating Karmøy from the mainland.

2.2 Challenges

In this study we have conducted all measurements according to rules dictated by previous modeling since our profile crosses 5 marine straits. Detailed sea water resistivity and depth measurements have been conducted and subsequently utilized in data processing. However, the highly conductive sea water (resistivity 0.20 Ωm) and strongly resistive bedrock (5000 Ωm and more) have rendered our measurements extremely noisy and hard to process. Interpretation of the 2D resistivity profile was aimed at discarding artificial effects (i.e. false anomalies which do not correspond to any real underground features) before making any final assessment.

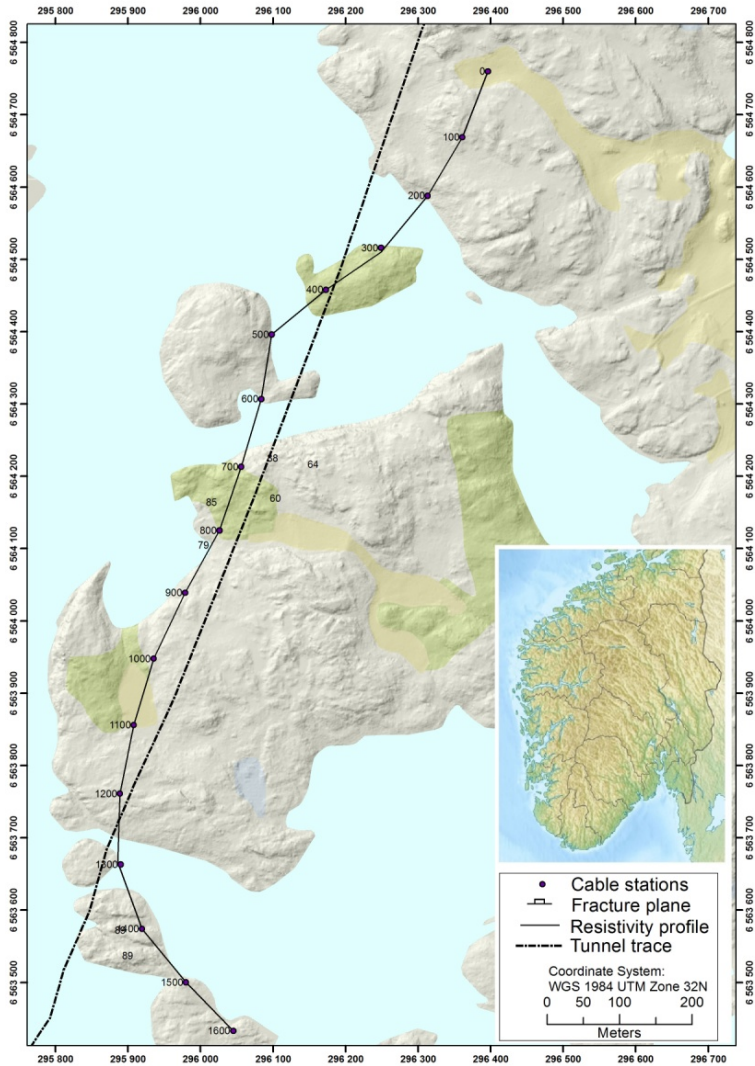


Figure 2: Geographical positioning of the profile with respect to the scheduled tunnel route.

As easily understood, the biggest problem in marine ERT is caused by the seawater conductivity itself but its depth is also a crucial factor in the success of such a survey. Prior modeling has shown that both floating and sea-bottom electrode modes can be successful for a limited depth extent. This limit was determined to be at 10 meters for sea-bottom and at 5 meters for floating electrodes. The detailed depth measurements that we have conducted in the region (which will be presented in detail in one of the following sections) revealed that the maximum thickness of the seawater along the profile was 4.6 meters. Essentially this means that we are within the aforementioned limitations and therefore marine ERT is applicable in this region. However, one can easily notice that 4.6 meters isn't much smaller than 5 meters when floating electrodes are employed. Consequently floating electrode measurements are expected to be less successful than sea-bottom mode especially if we consider the fact that the theoretical limits we have acquired via modeling were produced for a less conductive seawater and a less resistive bedrock.

In our modeling (Tassis et al 2013), we found that good performance of the resistivity method in marine environment were strongly dependent on seawater resistivity. In accordance with this and based on research of the available literature, we have used $0.25 \Omega\text{m}$ as a standard resistivity for seawater. Nevertheless, our measurements showed that the seawater resistivity in the area is even lower and equal to $0.2 \Omega\text{m}$, a feature which is expected to present a greater challenge for successful results.

Lateral effects caused by the sea water present a new challenge with the measurements at Arsvågen. So far, we have done 2D modeling which has used formations whose dimensions extended infinitely in the lateral direction. Nevertheless there are parts of our profile which do not fulfill this theoretical assertion. **Figure 2** shows the geographical positioning of the profile where we can see that there are several areas where despite our electrodes being on dry land, sea water is close by at a distance much smaller than the total length of the electrode spread. This special setting is strongly affecting our measurements due to the fact that the neighboring sea water offers the current an alternative and easier lateral route instead of the vertical one which has to penetrate a much more resistive bedrock. In other words, we are facing major underestimation of measured resistivities which does not reflect the real underground conditions. In order to go around this problem and pinpoint systematic artificial effects, 3D modeling is required. Unfortunately, the commercial 3D modeling software available offers limited possibilities and therefore can only give vague answers at this point, especially for the case of sea bottom electrodes.

3. METHOD DESCRIPTION

3.1 Method outline

The 2D resistivity method is based on the hypothesis that the distribution of electrical potential in the ground depends on the electrical resistivities and distribution of the surrounding geological formations. A geoelectrical survey is carried out by inserting an electrical current of known amplitude into the ground with the use of two electrodes and then by measuring the resulting voltage of the potential difference between two other electrodes (**figure 3**). Theoretically all electrodes should be aligned however, errors in positioning are common and difficult to avoid in real conditions. Theoretically, the signal is stronger compared to the ambient noise when the two potential electrodes are positioned between the current electrodes (nested arrays). However, electrode positioning which does not satisfy this setting, may be more appropriate for more sophisticated targets. In other words, the

positioning of electrodes i.e. the array used is governed by the targets that one wishes to detect.

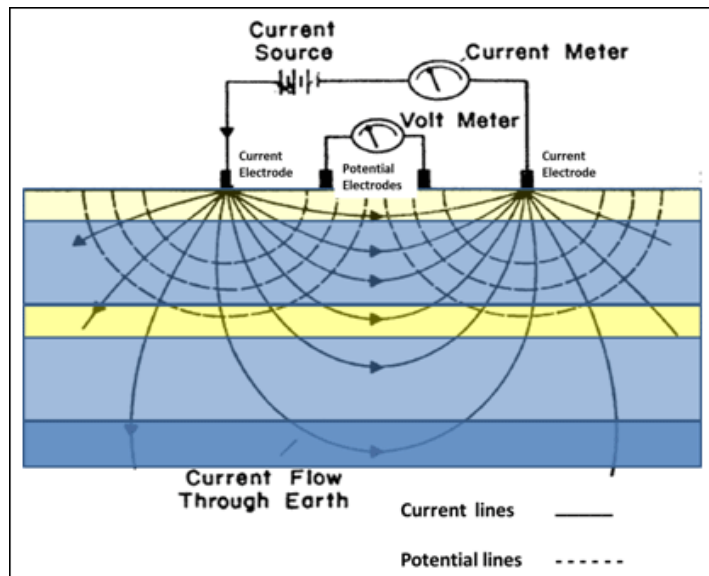


Figure 3: Electrode array for measuring the ground resistivity (modified by Todd 1959).

By changing the distance and positioning between current and potential electrodes we are able to produce a 2D pseudosection which comprises of a number of point measurements (figure 4). Using Ohm's law the measured resistance is easy to extract however, this quantity is not the one used for processing since we also have to take into account the geometrical characteristics of our electrode setting during acquisition. To count that in, we must multiply measured resistance with a K factor which is dependent of the electrode positioning of each individual measurement. Thereby we transform resistance into apparent resistivity. We use the term apparent to showcase that these are not the true resistivities of the underground formations but the average of the resistivities of the additional layers in a non homogeneous earth.

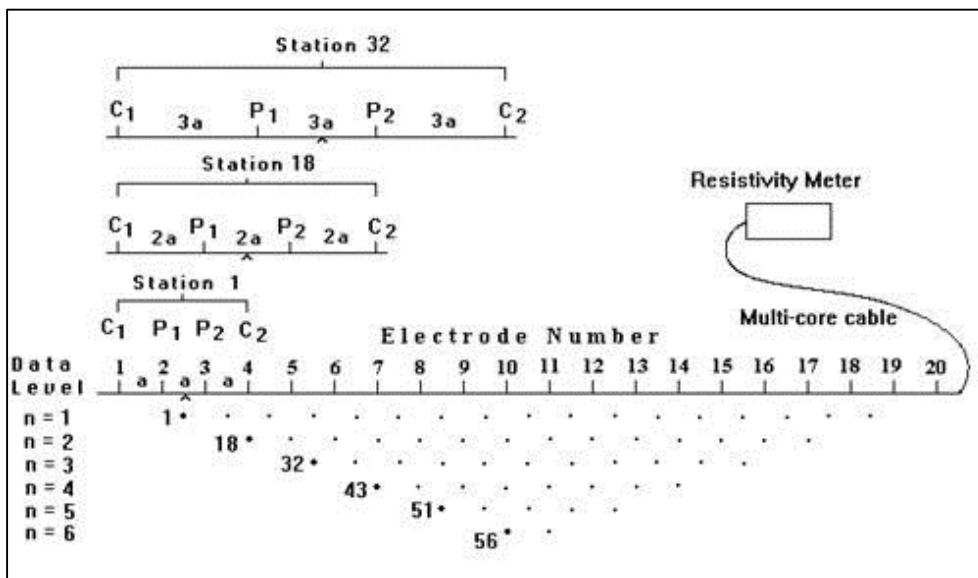


Figure 4: Sequence of measurements and structuring of a pseudosection (Dahlin 1993).

In this survey we have conducted 2D resistivity and induced polarization (IP) measurements. However, the presence of sea water has rendered our IP measurements unprocessable but also added a high noise level to our 2D resistivity ones.

3.2 Resistivity data acquisition

Electrical resistivity measurements have been collected with an array setting that has been developed at the Faculty of Engineering in Lund, Sweden and is known as the Lund system (Dahlin, 1993). This was done so with the use of a state-of-the-art electrical resistivity measuring instrument called the ABEM Terrameter LS (ABEM, 2012). This instrument has a strong transmitter and a high resolution 64 channel receiver which allows us to use 4 multi-electrode cables with 5 meter spacing simultaneously and perform measurements according to the Lund system setting (multiple gradient array - Dahlin and Zhou 2006).

The placing of electrodes and the sequence of measurements is shown in **figure 5**. As can be seen, we may extend our profile for as long as we choose by moving the first cable at the end of the array every time we have finished a measuring set. This method of extending a profile's length is called roll-along. In this survey we have performed this cable shifting 13 times in order to achieve the desired total length of 1600 meters. Each profile's true position has been measured with GPS. The GPS coordinates are shown in **Appendix 1**.

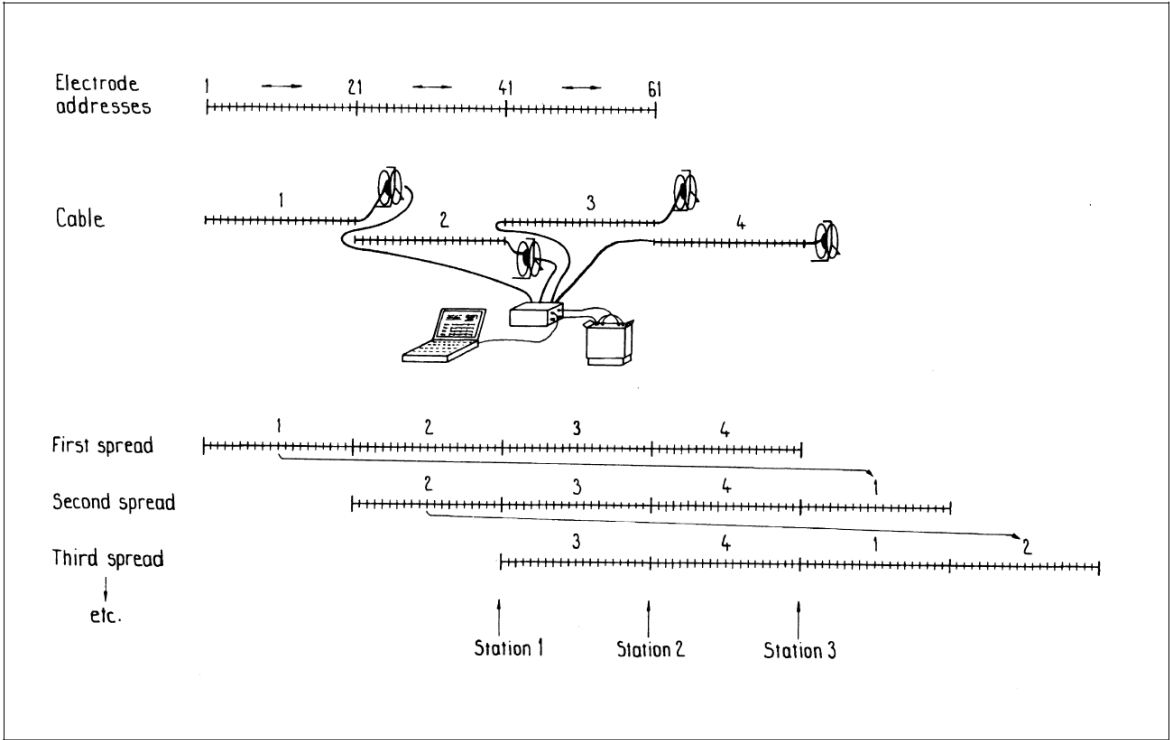


Figure 5: Diagram of measuring procedure. When measurements with four cables are terminated the first cable is moved at the end of the outlay to continue measurements as far as it is required (From Dahlin 1993).

As already mentioned, the northern 800 meters of the profile have been surveyed with three different arrays (multiple gradient, dipole-dipole, pole-dipole) in both sea-bottom and floating electrode mode. The measurements have been conducted in sequence for all settings after each spread (400 meters) was completed . The total datasets completed for each spread was

six: three arrays measured for sea-bottom and three arrays measured for floating electrode mode.



Figure 6: Floating electrode mode with the use of empty canisters along a strait in Arsvågen.

In practice, floating electrode mode was achieved with the use of custom floaters (empty canisters - **figure 6**) attached to every electrode outlet of the cable while sea-bottom mode was achieved by letting the cable sink on its own weight until the outlets contacted the sea bottom directly (**figure 7**).



Figure 7: Sea-bottom electrode mode with the cable sinking to the sea bottom on its own weight.

Measurements for different arrays have been performed with the use of protocols of the ABEM LS instrument. These protocols are files containing information about which electrodes are going to be used by the instrument to insert the current into the ground and which electrodes will be used for potential difference measurements. Therefore, measurements according to each array are controlled and carried out by the instrument itself.

3.3 Measurement parameters

Current for the largest part of our measurements varied around 200 mA. However, data quality was seriously degraded in the subareas of the profile where sea water was either present or close by. Raw data in these localities are characterized by several negative and close to zero measured resistivities which cannot be processed and need to be removed.

For the processing of data we are using Res2DInv version 4.03.32 (Loke, 2014a) which is the most commonly used software for this kind of surveys and it offers the possibility to switch the electrode positioning automatically whenever a negative value is found in the data. It also offers the possibility to make these measurements coherent with the geometrical factor and thus invert their sign from minus to plus. We have used both these options in processing the data.

As we can see from **figure 1** our entire profile is situated on top of the local highly resistive diorites which is the only major bedrock type present in our study area. This highly resistive bedrock combined with the extremely conductive sea water creates an environment which is not in our favor when trying to detect underwater fracture zones. The presence of sea water in the vicinity of such resistive bedrock (especially along the parts of our profile located on islands) affects our measurements laterally in the sense that the water offers the current a lateral route which is easier to follow than the expected vertical. This is due to the fact that the sea water in the neighborhood of our profile can be found at a distance radius much smaller than the total length of a single spread of each measurement set (400 m) thus including areas of saline water within each measurement's influence volume. Undershooting is therefore expected i.e. lower calculated resistivities than the actual bedrock values especially under the straits and islands of the profile.

Since most of the negative values are concentrated beneath sea water areas where our data sensitivity is high, their removal would mean a removal of 1438 values out of 6936 points in total. This would automatically degrade our resolution beneath all marine areas and make the detection of fracture zones in these localities even more difficult. Therefore, we have chosen to use the aforementioned modes in order to maintain an acceptable resolution in the sea bottom underground areas however, there is no way of indicating which of these values are erroneous and their negative sign is not due to the direction of the current. IP data were also very noisy and in some areas completely unprocessable. Therefore we decided not to present them in this report.

3.4 Seawater conductivity and depth measurements

In order to be able to process marine ERT data, detailed information about the seawater resistivity and depth should be available. Our profile crosses several straits and marine areas therefore such information is also necessary before any processing takes place. In Arsvågen we have acquired this information with the use of a WTW Conductivity Meter available from

Geotech Environmental Equipment and a custom made measuring tape relay with a small weight attached to its end in order to be able to sink down to sea bottom.

Both conductivity and depth measurements were made every 5 meters, at the exact positions where electrodes should be if the survey was done on dry land (**figure 8**). The depth was determined by sinking the measuring tape until the weight attached to it contacted the sea bottom and subsequently reading the indication on the plastic tape above the sea surface. Conductivity on the other hand was measured in a slightly more sophisticated way. The WTW Conductivity Meter is equipped with a sensor which is attached to a 3 meter cable. This cable has been marked with 1 meter notches which allows the user to gather conductivity readings from several different depths. Although the maximum depth in the region is closer to 5 meters, we have tried to use this feature and determine how seawater conductivity varies with depth down to at least 3 meters. Our field measurements indicate that seawater conductivity in our survey area varies imperceptibly between 47.6 to 48.8 mS/cm both in depth but also along the profile. These values transformed into the resistivity units used in ERT prospecting show local variations of only 0.001 Ωm , changes that can have no impact on the following inversion process. Therefore, we have used a rounded resistivity value of 0.20 Ωm which is perfectly fine for our calculations and accurately representative of the saline environment we are measuring in.

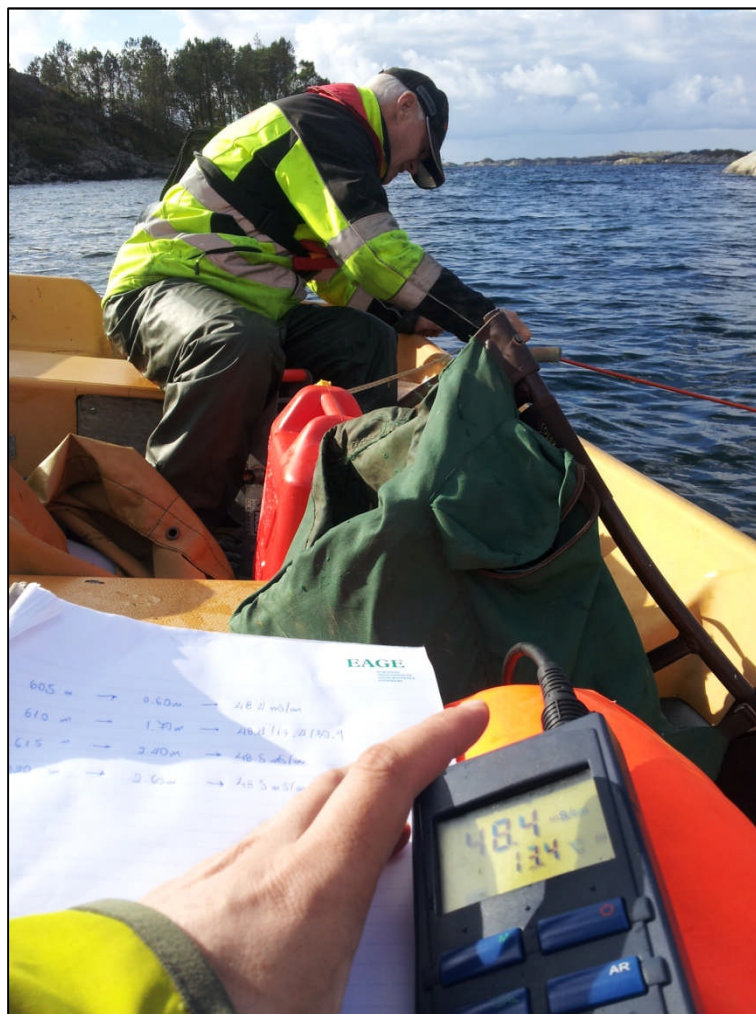


Figure 8: Field measurements of sea water depth and conductivity/resistivity.

This information was subsequently used in order to fix the properties of the seawater layer prior to inversion. In the case of sea-bottom electrodes Res2DInv offers a module to automatically fix the seawater layer but in the case of floating electrodes, this had to be done indirectly. This means that in order to fix the sea layer we had to break down each seawater body into rectangulars and triangles and assign a singular resistivity value to it.

3.5 Inversion

The measured resistivity is essentially an apparent resistivity which represents a weighted mean of all resistivities that are within the measurement's influence volume. To find the true resistivity in different parts of the subsurface we must invert our data. This is accomplished by dividing the ground into blocks and assigning a specific resistivity to each one of them. This model is then adjusted in several intermediate steps (iterations) until the response from the theoretical model matches the measured data as much as possible.

As already described inversion was done with Res2DInv software. Prior to inversion all sea water areas were fixed accordingly to our measurements i.e. where assigned their true geometrical dimensions and resistivity which were not allowed to change throughout the inversion. Attempts were made with different inversion methods (standard Least-Squares, data and/or model robust, fast inversion, model discretization) and we also experimented with several different inversion parameters such as different damping factors and vertical/horizontal filters. We have decided that the best processing scheme includes robust data inversion in fast mode with prior model discretization. Damping factors were not increased before the inversion process while the Vertical/Horizontal filter was raised to 1.5 in order to favor vertical structures.

4. RESULTS AND DISCUSSION

Resistivity contrasts

The inversion results are presented in **figures 9, 10** and **11** for the first 800 meters of the profile and **figure 12** for the entire 1600 meters of the cross section. The calculated resistivity distribution (inverse of electrical conductivity in the bedrock) is shown in the colored section of the profile where each color corresponds to a specific value range. Resistivity varies between low values which are shown in blue and green (1-500 Ωm) to higher values which are shown in brown and red ($> 5000 \Omega\text{m}$). Brown and red indicates generally massive bedrock, while blue/green indicates either weak bedrock or soil. Topography was also taken into account during inversion and plotting and we have used a distorted finite-element grid with damped distortion (distortion factor: 0.40). Moreover, the fixed marine areas are shown in deep blue color to indicate their measured resistivity of 0.20 Ωm according to the color scale. Their geometrical outline can also be seen wherever this is possible due to the vertical imaging scale (mean sea level at 0 meters).

Inversion parameters

For the inversion we have used a refinement option which is called model discretization and handles data as if half the electrode spacing had been used. This is increasing the resolution on the shallower layers of our cross section where data are more reliable than in larger depths. As for the robust inversion module, we have chosen to use the robust data constraint which makes the inversion process less sensitive to noisy data such as our own but not the robust model constraint in order to maintain detail as high as possible in the resulting image especially below the marine areas. That is also the reason why we did not use increased

damping factors. A fast inversion module was also chosen in order to speed up processing time without any major impact on the results. Finally, the Vertical/Horizontal filter in most of our results is equal to 1.0 however, the 1600-meter profile in **figure 12** has also been inverted with a V/H filter equal to 1.5 in order to enhance any vertical structures.

Noisy data

Our first assessment on the results is that we are dealing with extremely noisy data, a fact highlighted by the high error value of our calculations in all figures. The error varies in respect with the array employed and whether we are using sea-bottom or floating electrodes from 34,2 to 82,2%. **Figures 9, 10 and 11** clearly prove that the use of sea-bottom electrodes is superior to floating electrode mode. Not only do we calculate lower inversion errors but also the images we extract are more coherent with more detailed information below seawater regions. However, even in the best of cases (**top side figure 9** - multiple gradient array/sea-bottom electrode mode) this error is almost 10 times larger than the error of a typical dry land survey. Furthermore, the presence of sea water is causing systematic artificial effects in the inversion results. These effects vary from fracture-zone looking anomalies at the edges of all marine areas when multiple gradient and dipole-dipole arrays are employed to huge low resistivity areas which cover the entire underwater sub region when pole-dipole array is used.

Electrode configurations

Theoretically, all images extracted from different arrays should be coherent to each other and portray similar structures but in Arsvågen this is not the case. The high errors of all three arrays but especially the one of dipole-dipole (**figure 10**) indicate that these results are already not accurate enough standalone and therefore cannot be compared to each other safely. Each individual profile is strongly dependent on the way that the measurements are being taken in connection to the theoretical background of each array and the instability of the inversion process itself. How the highly conductive seawater affects each array is not clear enough to us but error-wise, dipole-dipole seems to be the noisiest of them all. According to modeling results (Tassis et al., 2014) dipole-dipole is one of the most successful arrays in marine environments regardless of its sensitivity to noise. Nevertheless, this theoretical conclusion refers to the optimal conditions we have chosen for modeling. In real conditions, the extremely conductive seawater decreases the already weak signal to noise ratio of the array further and pushes its results to unreliability even in sea-bottom electrode mode. A mathematical error of 63,7% is too high and forbids any type of conclusion extraction from the use of this array. Multiple-gradient and pole-dipole (**figures 9 and 11**) on the other hand seem to give relatively better results but their calculated errors are still very high (34,2 and 39,1% respectively). Between these two arrays, pole-dipole fails to retain any sort of detail below marine areas and presents a rather vague image as opposed to multiple gradient which regardless of artificial effects, shows a more detailed variation below seawater. Therefore, it is safe to assume that none of the additional arrays would give any better results or more insight on possible underwater fracture zones than multiple gradient for the entire profile. For this reason, resuming the entire profile with multiple gradient array and sea-bottom electrode mode was indeed the most precise approach.

Artificial effects

It should be noted though that regardless of the fact that multiple gradient seems to be working better in these extreme conditions, still it is plagued by several artificial effects which could be mistaken for anomalies. These anomalies are located on the edges of all marine areas and have a resistivity which varies mainly between 5 and 20 Ωm but locally becomes even lower. Low resistivity areas are found beneath all marine areas whose shape and form is dependent on whether we are dealing with an island or a mainland shore. For example, at 215

meters of horizontal distance (see **figure 9**) there is a low resistivity area which does not extend in depth. We believe this is due to the fact that north of this point lies the Bokn mainland. At 285 meters on the other hand, we can see a low resistivity fracture zone-looking anomaly which extends towards depth and widens significantly at about 40 meters. In this case we believe that the anomaly continuation towards the depth is due to the fact that south of the aforementioned point lies the first island we have encountered in our survey. This pattern seems to be valid throughout the profile. Wherever the sea meets the mainland we observe the aforementioned type of superficial low resistivity anomalies (215, 670, 1270 meters). It may also be useful to note that the observation made above is also valid between 1030 and 1100 meters where a bog containing mainly fresh water of 20 centimeters depth is found. Anomalies on either side of this swampy area are also limited to the superficial part of the underground, as is the case in all the aforementioned localities. On the contrary, in places where the sea meets an island the anomalies tend to extend in depth (285, 440, 490, 605, 1340 meters). Summarizing, we believe that all these anomalies do not represent real fracture zones. Still, there is always a chance that the presence of an actual fracture zone in these points could be shadowed by the aforementioned effect.

3D effects

Another interesting feature of the inversion result is the low resistivity areas beneath all the islands and near the maximum penetration depth of the method (~70 m), an effect which starts shallower and is more severe with dipole-dipole and pole-dipole arrays (**figures 10** and **11**). As shown in **figure 1** the survey crosses 3 islands in total, two in the north and one in the south. The effect described above is present in all three localities. The anomalies located at the edges of the watery areas extend towards the depth and connect to create a low resistivity formation which starts off below the islands at about 200 Ωm and becomes as low as 5 Ωm at maximum depths. An educated explanation for this effect could include the presence of sea water at a close distance whenever a measurement takes place on an island. In most cases the sea water can be found at maximum 50 meters of lateral distance, which is comparable to the maximum penetration depth of our array. This means that the influence volume of each measurement includes a various amount of sea water which in turn decreases the value of the mean measurement resistivity. This effect was unforeseen during our 2D modeling due to the fact that all formations in a 2D model are thought to be extended to infinity towards the lateral direction. This means that in order to be able to imitate this effect accordingly to our survey area, we should perform 3D modeling with an increasing amount of sea water present nearby. Therefore, these deep low resistivity anomalies are most probably artificial effects since only massive bedrock can be expected in such extent and depth on a strict geological sense. For this purpose we have chosen to present only the upper part of the 1600-meter profile (until 50 meters of penetration depth) in order to exclude these low resistivity areas from the final results. A low resistivity formation at a depth of 70 m in an area dominated by high resistivity bedrock has no physical meaning therefore it could be safely discarded. Regardless of whether this effect is due to our measured data or the inversion process itself, depths below ~40-50 meters are not included in **figure 12**.

Bathymetric effects

The above described pattern also allows the middle parts in most of the marine straits to acquire resistivity values which are typical for bedrock, an indication which could also mean that no fracture zone is present in these localities. The first and last strait in the area however, have a special bathymetry in which the sea bottom rises at 260 and 1305 meters to create a bump that separates the straits into two sub-straits. In both cases these bumps are characterized by low resistivities (~20 Ωm) while weak bedrock resistivities are calculated on either side of them (500 Ωm or more). This could be indicative of the presence of a fracture

zone in these areas however, once again we should be suspicious that this is a repeated effect and not a unique appearance. In a sense, these bumps could be considered as small islands which as mentioned above could satisfy the conditions for the calculation of two false anomalies on either side of them which are extending in depth. Nevertheless the dimensions of these small islands do not allow these two artificial effects to become separated therefore they appear as one elongated low resistivity area. Consequently, assigning fracture zones to these anomalies is again dubious at best.

Real structures

The only fracture zones which we could pinpoint in the map would be of course located on top of dry land areas. In accordance with **figure 1** where superficial traces of fracture zones have been identified with field mapping and are also plotted, a prominent almost vertical low resistivity anomaly can be seen at 1400 meters. Moreover, a new tectonic map of the region conducted by the geologists of the NGU indicates that a possible lineament is crossing the first strait in the north. Therefore there is a possibility that a fracture zone might be there whose blueprint is being shadowed by artificial effects caused by the sea bottom bump. However, we should always keep in mind that assessments referring to areas beneath sea water are ambiguous and the risk of them proving false is high.

In today's market one can easily find specially designed instruments for marine ERT measurements. Those instruments' main characteristic is that they are more powerful than usual ERT equipment, which means that they can handle stronger electrical currents and can subsequently insert more current into the ground. The NGU doesn't own such an instrument therefore the intensity of the current we have used is lower than the one those instruments can employ. However, a stronger current does not decrease the percentage of current loss in the seawater, since the ratio of the current that infiltrates the ground to the current lost in the sea will remain constant. Ohm's law dictates that resistance can be calculated by dividing potential with current. Therefore, a higher current will result in a proportionately higher measured potential and if we divide those quantities, their proportionate higher levels will be annulled resulting in the same calculated resistance (or resistivity) as in the case of less powerful currents. Nevertheless, a high-current feature like that can prove useful in cases where the measured resistance is close to the noise level and we need to boost our signal above it. In our case, we believe that the artificial effects, induced to our data by the extreme resistivity difference between bedrock and seawater shields and overshadows all these near null measurements that a higher current could reveal. The ambiguity of our results is not due to a weak current but due to the geometry of the study area and weaknesses in inversion software. Of course, this matter could be resolved with 3D modeling but until we have the opportunity to do so, we cannot draw any safe conclusions.

Alternative inversion software

It should be noted that we have requested two geophysicists with expertise in ERT to process our data with their own inversion programs in order to evaluate Res2DInv results but both failed. The extreme difference in resistivity between bedrock ($>5000 \Omega\text{m}$) and seawater ($0.20 \Omega\text{m}$) caused the aforementioned codes to calculate extreme values which then caused the inversion code to crash after a number of iterations. In this sense, we acknowledge that the conditions in the area are not favorable regardless of the fact that the results of our 2D modeling indicate that the lowest acceptable standards are fulfilled. Unfortunately 2D modeling is not enough to help us identify artificial effects in such a survey.

5. CONCLUSIONS

Our inversion results have generated more questions than answers about the feasibility of 2D resistivity method application in an environment containing islands. These questions mainly refer to the lateral effects to our measurements caused by the existence of highly conductive sea water in the vicinity of our profile and artificial effects caused by the inversion software. We have tested two other inversion codes, but both failed probably due to extremely high resistivity contrast.

3D modeling could clear up several issues connected to false low resistivity anomalies which appear systematically in our results. Nevertheless, the existent software available to the NGU does not cover the case of sea bottom electrodes. Requests have been made in order for such an option to become available with the Res3DMod software (Loke, 2014b) but it has not been answered yet. Resolving of this matter will require time which exceeds the report deadline.

What we are dealing with is a complex geophysical problem that hasn't been addressed by the scientific community so far. Therefore resolving it, is dependent on the NGU for the time being. In order to do so, this requires further geophysical research efforts which will in turn give useful answers for future surveys. In any case the results are extremely noisy and unclear, especially for the conditions present in our study area.

We may have certified that multiple gradient array and sea-bottom electrode mode is the best possible configuration when surveying marine areas but we haven't been able to obtain clear enough results in order to make any kind of final assessment. The feasibility of ERT in marine environments which include islands is still in question.

To sort out either or not there are fracture zones in bedrock under the investigated straits at Årvågen, the NGU recommends to perform refraction seismic measurements. These measurements should be done along identical or at least neighboring to the ERT profiles. In this way, refraction seismic results can be directly compared to the ERT ones and possibly help us clarify some of the issues we have already addressed in this report.

To overcome 3D effects on the resistivity data on the other hand, NGU will perform new modeling and inversion when appropriate software is available.

Acknowledgements.

The authors like to thank *The Public Roads Administration; The Rogfast project* and *The Directorate of Public Roads* for financial support.

6. REFERENCES

- ABEM, 2012: ABEM Terrameter LS. Instruction Manual. ABEM 20120109, based on release 1.10. ABEM, Sverige.
- Dahlin, T. 1993: On the Automation of 2D Resistivity Surveying for Engineering and Environmental Applications. Dr. Thesis, Department of Engineering Geology, Lund Institute of Technology, Lund University. ISBN 91-628-1032-4.
- Dahlin, T. and Zhou, B. 2006: Multiple-gradient array measurements for multichannel 2D resistivity imaging. *Near Surface Geophysics*, Vol 4, No 2, April 2006, pp. 113 - 123.
- Dalsegg, E. 2012: Geofysiske målinger på Kvitsøy, Kvitsøy kommune, Rogaland. NGU Report 2012.033.
- Elvebakk, H. 2011: Sammenstilling av resistivitet, seismiske hastigheter og naturlig gammastråling i norske bergarter; NGU rapport 2011.042.
- Loke, M.H. 2014a: RES2INV ver. 4.03.32. Geoelectrical Imaging 2D & 3D. Instruction manual. www.geotomosoft.com.
- Loke, M.H. 2014b: 3-D resistivity & IP forward modeling using the finite-difference and finite-element methods. Instruction manual. www.geotomosoft.com.
- Ragnhildstveit, J.; Naterstad, J.; Jorde, K.; Egeland, B. 1998: Haugesund. Berggrunnskart; Haugesund; 1:250 000; trykt i farger.
- Reiser, F., Dalsegg, E., Dahlin, T., Ganerød, G. & Rønning, J.S. 2009: Resistivity Modelling of Fracture Zones and Horizontal Layers in Bedrock. NGU Report 2009.070 (120 pp).
- Rønning, J.S. 2003: Miljø- og samfunnstjenlige tunneler. Sluttrapport delprosjekt A, Forundersøkelser. Statens vegvesen, Publikasjon nr. 102.
- Rønning, J.S., Dalsegg, E., Elvebakk, H., Ganerød, G.V. & Heincke, B.H. 2009: Characterization of fracture zones in bedrock using 2D resistivity. Proceedings from 5th Seminar on Strait Crossings, Trondheim, June 21 – 24 2009, p. 439 - 444 (SINTEF/NTNU).
- Rønning, J.S., Ganerød, G.V., Dalsegg, E. & Reiser, F. 2013: Resistivity mapping as a tool for identification and characterization of weakness zones in bedrock - definition and testing of an interpretational model. *Bull. Eng. Geol. Environment* Volume 73, Issue 4 (2014), Page 1225-1244
- Solli, A. 2014: Geological investigations for the ROGFAST project in the area between Kvitsøy and Bokn; NGU report 2014.054.
- Tassis, G.; Tsourlos, P.; Rønning, J.S.; Dahlin, T. 2013: Detection and characterization of fracture zones in bedrock in a marine environment - Possibilities and Limitations. NGU Report 2013.017 (77 pp.).
- Todd, D.K. 1959: Groundwater hydrology. John Wiley & Sons, Inc., New York.

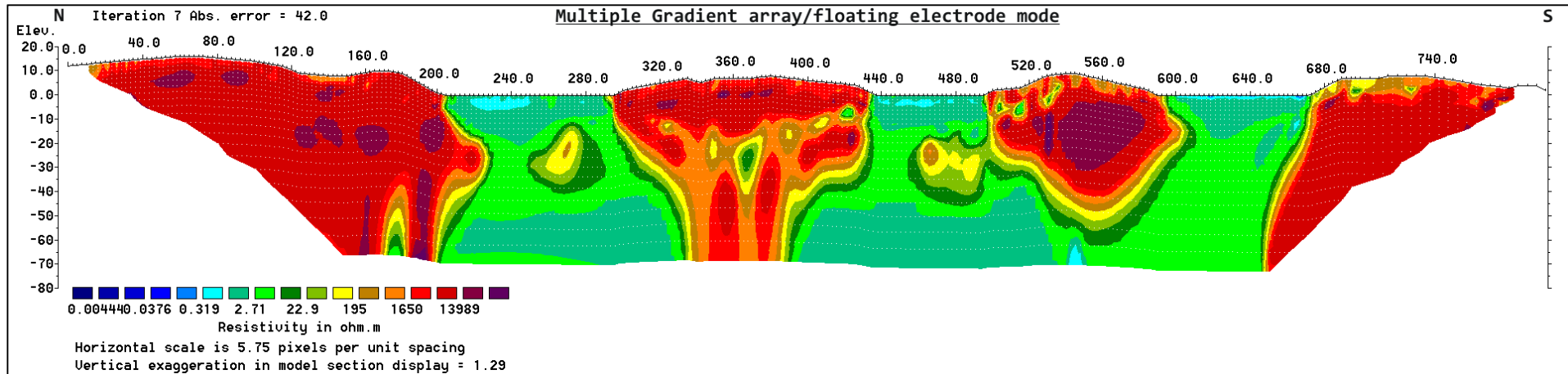
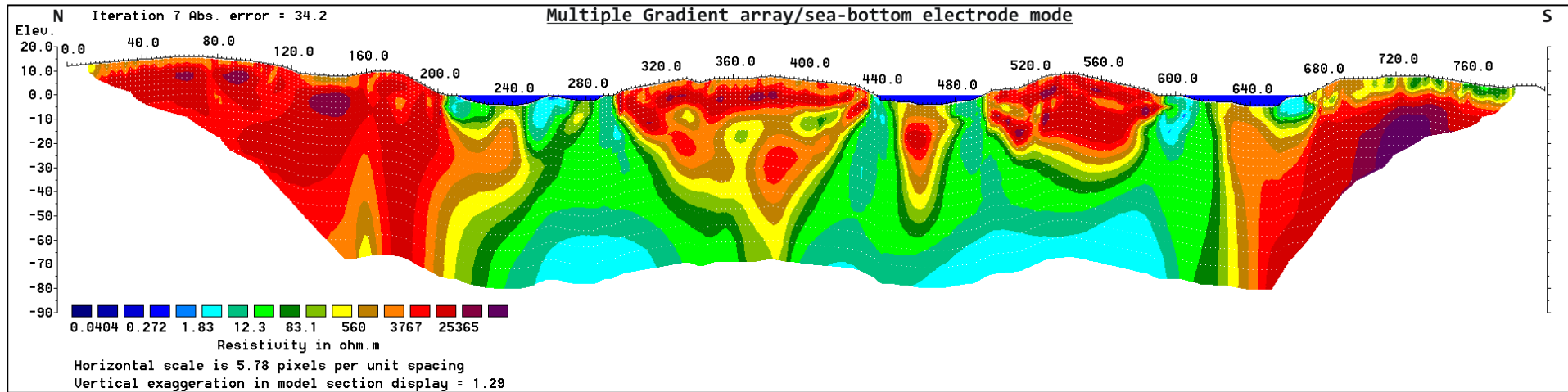


Figure 9: Modeled resistivity with topography for multiple gradient array on sea-bottom electrode mode (top side) and floating electrode mode (bottom side). Inversion parameters: Robust data inversion/Fast module, V/H filter = 1.5.

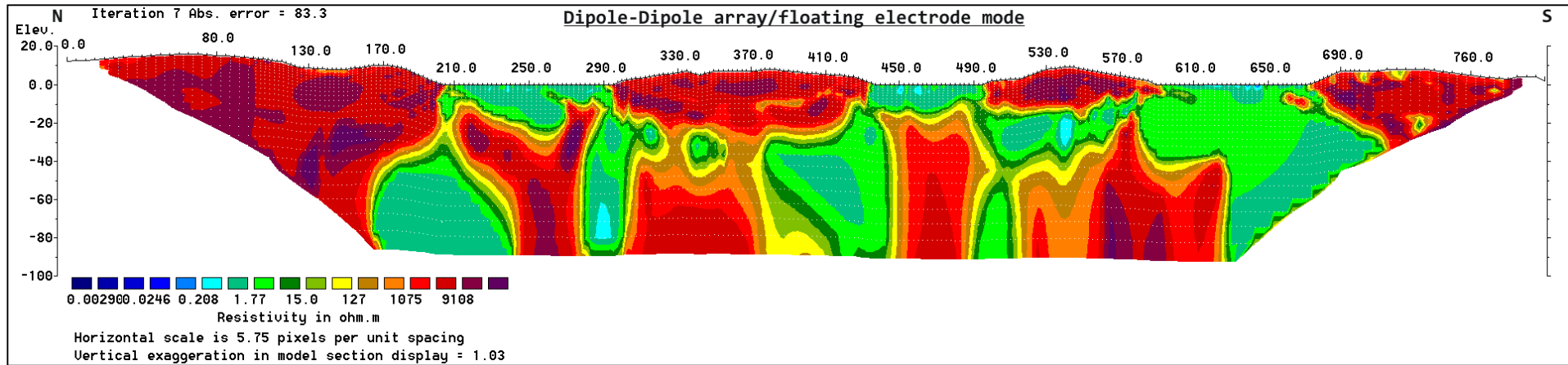
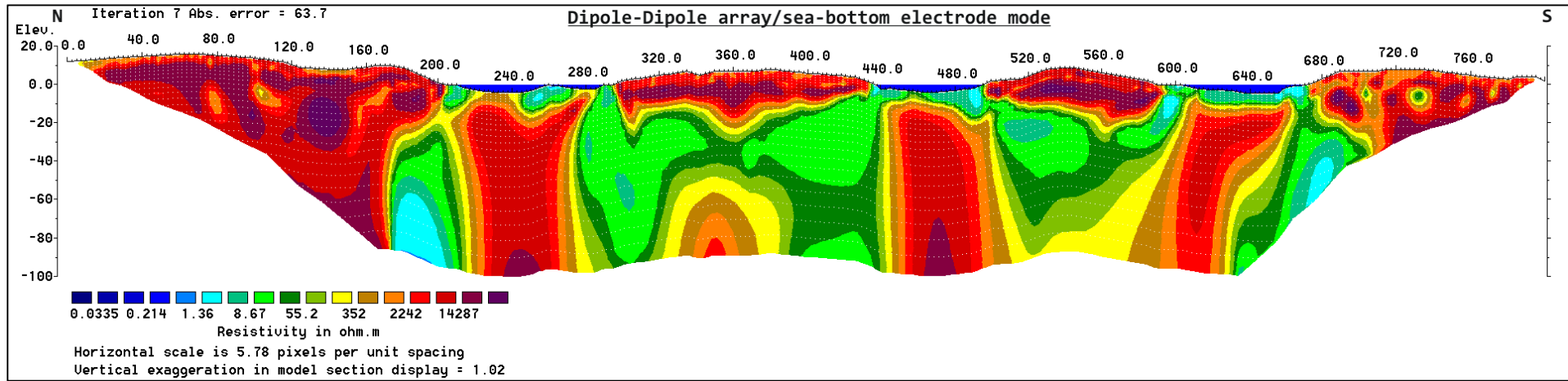


Figure 10: Modeled resistivity with topography for dipole-dipole array on sea-bottom electrode mode (top side) and floating electrode mode (bottom side). Inversion parameters: Robust data inversion/Fast module, V/H filter = 1.5.

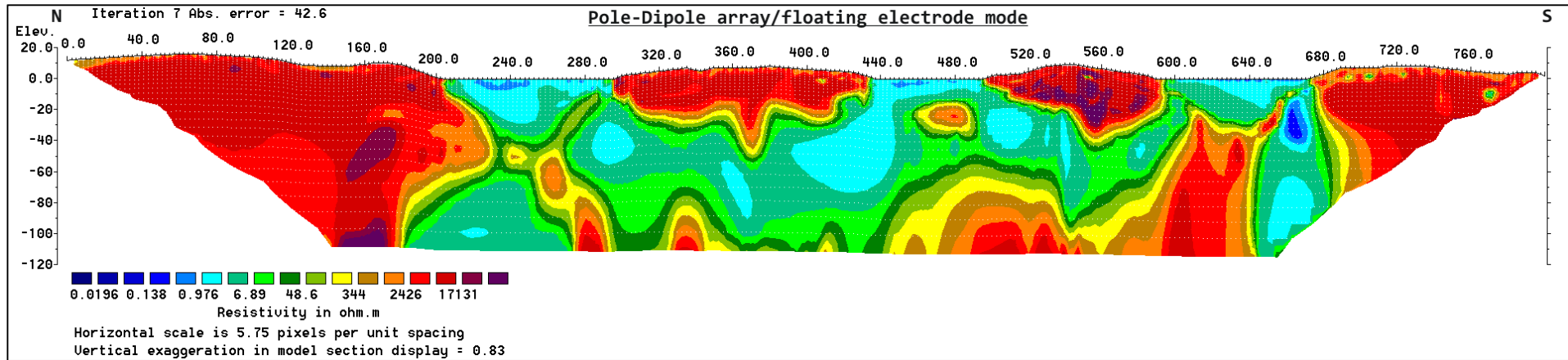
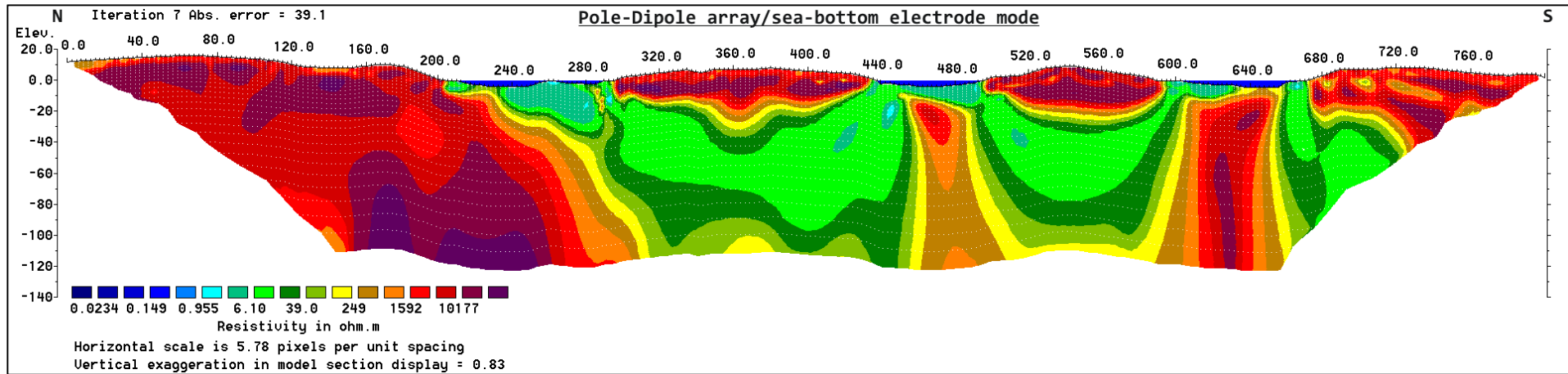


Figure 11: Modeled resistivity with topography for pole-dipole array on sea-bottom electrode mode (top side) and floating electrode mode (bottom side). Inversion parameters: Robust data inversion/Fast module, V/H filter = 1.5.

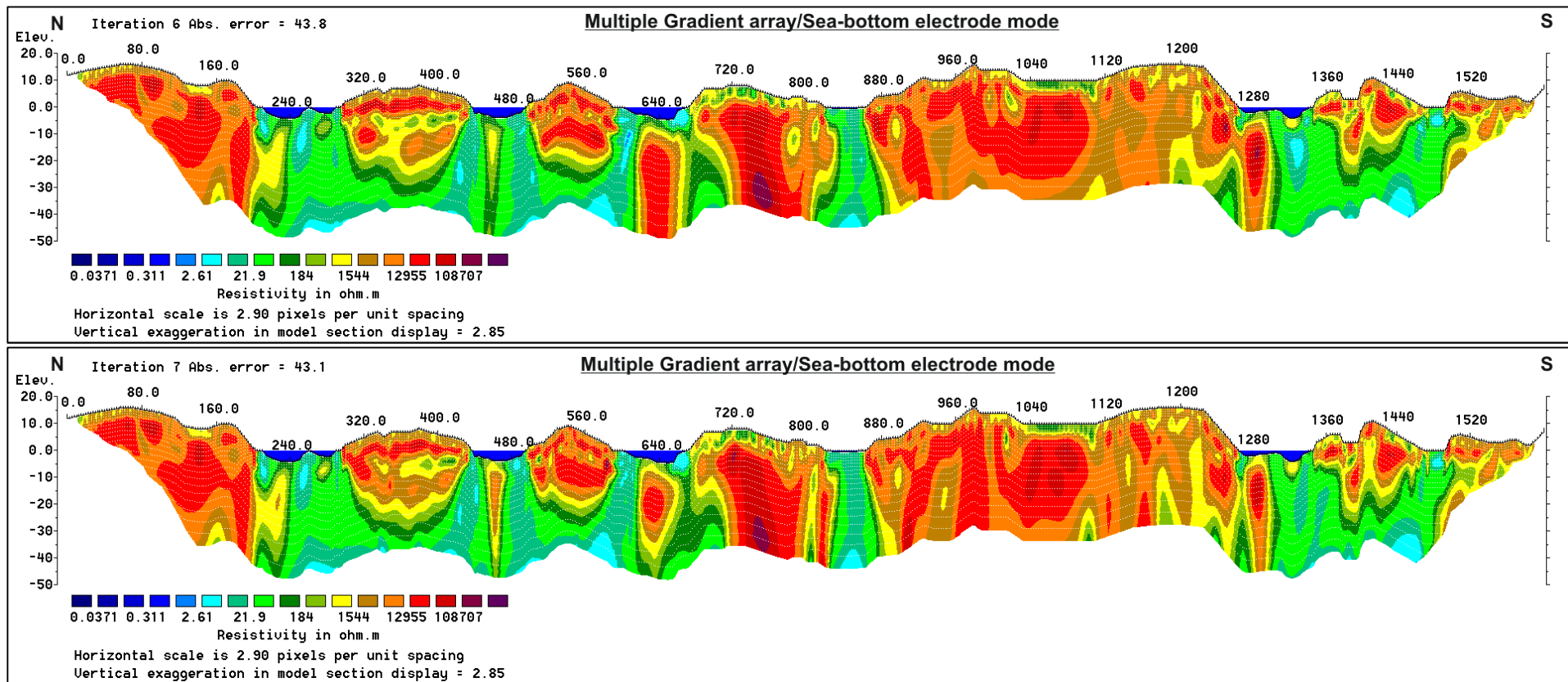


Figure 12: Modeled resistivity with topography for multiple gradient array on sea-bottom electrode mode with V/H filter equal to 1.0 (top side) and with V/H filter equal to 1.5 (bottom side). Inversion parameters: Robust data inversion/Fast module.

7. APPENDIX 1, Station coordinates

In UTM 32N/WGS 84.

Station	X (in meters)	Y (in meters)
0	296396	6564760
100	296361	6564669
200	296313	6564588
300	296249	6564516
400	296173	6564458
500	296098	6564396
600	296080	6564311
700	296056	6564213
800	296026	6564125
900	295979	6564041
1000	295929	6563944
1100	295908	6563856
1200	295889	6563761
1300	295890	6563663
1400	295929	6563944
1500	295980	6563500
1600	296045	6563433